Check for updates

HEMOGLOBIN DISORDERS

A tetramer of BCL11A is required for stable protein production and fetal hemoglobin silencing

Ge Zheng[1]†, Maolu Yin[1]†, Stuti Mehta[1]†, I-Te Chu[1], Stacy Wang[3], Alia AlShaye[1], Kirstin Drainville[1], Altantsetseg Buyanbat[1], Frédérique Bienfait[1], Karin Tenglin[1], Qian Zhu[3], Stuart H. Orkin[1,2]*

Down-regulation of BCL11A protein reverses the fetal (HbF, $\alpha_2\gamma_2$) to adult (HbA, $\alpha_2\beta_2$) hemoglobin switch and is exploited in gene-based therapy for hemoglobin disorders. Because of reliance on ex vivo cell manipulation and marrow transplant, such therapies cannot lessen disease burden. To develop new small-molecule approaches, we investigated the state of BCL11A protein in erythroid cells. We report that tetramer formation mediated by a single zinc finger (ZnF0) is required for production of steady-state protein. Beyond its role in protein stability, the tetramer state is necessary for γ-globin gene repression, because an engineered monomer fails to engage a critical co-repressor complex. These aspects of BCL11A protein production identify tetramer formation as a vulnerability for HbF silencing and provide opportunities for drug discovery.

During ontogeny, the principal hemoglobin in red blood cells changes from fetal (HbF, $\alpha_2\gamma_2$) to adult hemoglobin (HbA, $\alpha_2\beta_2$), paralleling a progressive cellular switch from fetal liver to bone marrow erythropoiesis (*1*). This developmental transition begins in mid-gestation and is completed during the first few months after birth. As the major hemoglobin disorders, sickle cell disease (SCD) and β-thalassemia are caused by mutations in the adult β-globin gene. Affected individuals are typically spared symptoms in the neonatal period, as first described for children with SCD 75 years ago (*2*). Recognition that the clinical severity of SCD and β-thalassemia is ameliorated by increased levels of HbF, resulting from either common genetic variation (*3*, *4*) or rare mutations in hereditary persistence of fetal hemoglobin (HFPH) syndrome (*5*, *6*), has fueled decades-long interest in the fetal-to-adult hemoglobin switch. Clinical observations have provided a compelling rationale for reactivation of HbF expression as therapy for the hemoglobinopathies. The barrier to accomplishing this goal was lack of knowledge regarding mechanisms underlying the process. Research over the past 15 years has provided an increasingly detailed view of how HbF silencing is controlled and may be targeted for therapeutic benefit.

At the molecular level, the fetal-to-adult hemoglobin switch reflects a switch in transcription from duplicated γ-globin genes to the downstream β-globin gene in the β-globin locus on chromosome 11. The repressor protein BCL11A, an adult-stage factor, is the principal physiological regulator of the switch (*1*, *7*). BCL11A acts directly at the γ-globin gene promoter by binding at a canonical DNA-recognition sequence (*8*, *9*) and displacing a ubiquitous transcriptional activator (NF-Y) (*10*). Engagement of the nucleosome remodeling and deacetylase (NuRD) complex by BCL11A is believed to contribute to repression at the locus (*7*, *11*). Shutoff of γ-globin gene transcription liberates a strong upstream enhancer, the locus control region (LCR), to loop to and activate transcription of the β-globin gene (*12*, *13*). A second, stage-independent repressor protein, ZBTB7A (LRF), also acts to silence the γ-globin genes by binding a site further upstream in their promoters (*8*, *14*).

Several findings have positioned BCL11A as a genetic target for therapeutic manipulation. Down-regulation of its expression in adult $CD34^+$ cell–derived erythroid precursor cells [hematopoietic stem and progenitor cells (HSPCs)] leads to increased HbF levels, demonstrating that γ-globin silencing is reversible and dependent on BCL11A (*7*). Indeed, subsequent observations have revealed that the level of BCL11A dictates the level of HbF at the adult stage. Modest decreases in BCL11A expression that result from common genetic variants in an essential erythroid-specific enhancer within the gene itself (*15*), first identified through genome-wide association studies (*3*, *4*), are associated with small but consistent increases in HbF levels (~1 to 3%) in the population. In individuals with neurodevelopmental deficits due to a rare BCL11A haploinsufficiency syndrome, HbF levels are much higher (~15% on average) (*16*). Within HSPCs, the extent of increased HbF expression strongly correlates with the reduction in BCL11A expression (*17*). In effect, BCL11A serves as a rheostat for HbF. Besides this dose sensitivity, marked down-regulation of BCL11A alone is sufficient to reactivate HbF expression to generally accepted therapeutic levels (~30% total Hb per red blood cell), as first revealed by genetic rescue of engineered SCD mice (*18*). The discovery that CRISPR-Cas9–mediated disruption of a single GATA1 binding site in the BCL11A erythroid enhancer greatly impairs BCL11A expression (*19*, *20*) has been translated in trials of patients with SCD and β-thalassemia with transformative clinical outcomes (*21*), culminating recently in regulatory approval of the first gene editing therapy, Casgevy. A notable feature of both rescue of engineered SCD mice and success of Casgevy is the tolerance of red blood cell differentiation and production to low levels of BCL11A. This relative insensitivity likely reflects the few primary gene targets for BCL11A in erythroid cells, as revealed by nascent transcript analysis after acute protein depletion (*22*).

Besides providing a transformative therapy for patients, the success of gene editing (*21*), taken together with a trial of short hairpin RNA (shRNA)–mediated down-regulation of BCL11A in patients with SCD (*23*), establishes BCL11A as a clinically validated therapeutic target for HbF reactivation. As currently practiced, genetic therapies cannot be delivered to large numbers of patients because of the cost and intensive care required. Unless methods for in vivo delivery of gene-based therapies become efficient enough to modify a substantial fraction of host hematopoietic stem cells, small-molecule drugs will be required to reduce overall disease burden. Whereas modulating epigenetic pathways has been pursued as a route to therapeutics (*24*–*29*), the direct involvement of BCL11A in γ-globin repression and its validation in the clinical setting provide a compelling rationale for targeting the protein itself.

By studying structure-function relationships, we explored how the BCL11A protein is processed and functions in erythroid cells. Steady-state BCL11A protein requires formation of a tetramer, which is mediated by a single zinc finger (ZnF0) near its N terminus. Apart from its role in protein stability, the tetramer state itself is critical for γ-globin repression. Our findings present potential opportunities for therapeutic targeting of BCL11A.

Results

ZnF0 mediates multimeric interactions and is required for steady-state protein expression

BCL11A contains seven ZnF domains, numbered from 0 to 6 (Fig. 1A). ZnF0 is a C2HC ZnF, whereas ZnFs 1 to 6 are of the more common C2H2 class. A canonical peptide sequence at the BCL11A N terminus binds RBBP4, a subunit of the NuRD complex (*30*–*32*). C-terminal ZnF456 recognize and bind the sequence TGACCA in the γ-globin promoters (*9*). As predicted by PONDR (prediction of disordered regions) (*33*) and AlphaFold 3 (*34*), BCL11A is largely disordered, except for its ZnFs (fig. S1, A and B). In

[1]Dana-Farber/Boston Children's Hospital Cancer and Blood Disorder Center, Department of Pediatrics, Harvard Medical School, Boston, MA, USA. [2]Howard Hughes Medical Institute, Harvard Medical School, Boston, MA, USA. [3]Lester Sue Smith Breast Center, Department of Human Molecular Genetics, Baylor College of Medicine, Houston, TX, USA.
*Corresponding author. Email: stuart_orkin@dfci.harvard.edu
†These authors contributed equally to this work.

Downloaded from https://www.science.org at University Van Amsterdam on April 13, 2025

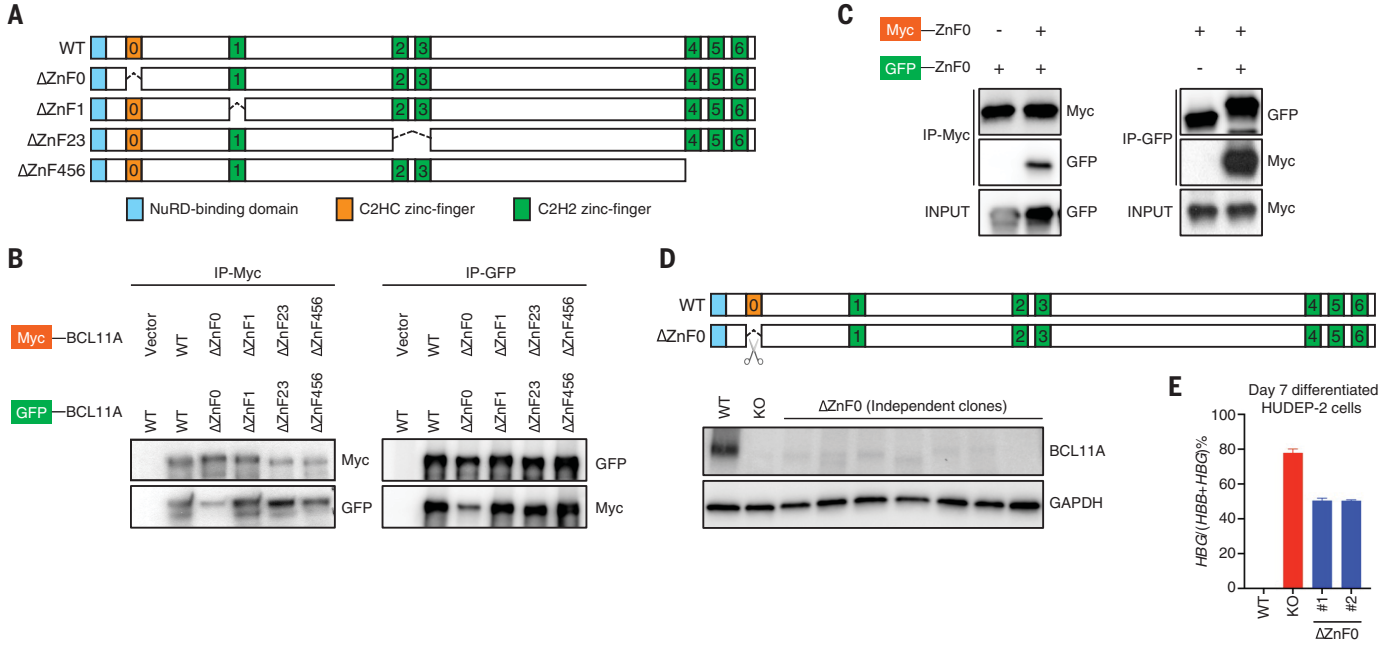

Fig. 1. ZnF0-mediated multimeric interaction is required for BCL11A steady-state protein level. (**A**) Schematic of BCL11A constructs lacking individual zinc fingers or zinc finger clusters. Constructs were expressed with Myc or GFP epitope tags and transfected into HEK293T cells for reciprocal immunoprecipitations. (**B**) Anti-Myc and anti-GFP immunoprecipitates (IPs) were Western blotted with indicated antibodies in HEK293T cells cotransfected with indicated plasmids. Myc- or GFP-tagged BCL11A lacking ZnF0 failed to multimerize with each other. (**C**) Total cell lysates (INPUT) and anti-Myc and anti-GFP IPs were blotted with the indicated antibodies in HEK293T cells cotransfected with the indicated plasmids. ZnF0 alone was sufficient to mediate multimer formation. (**D**) HUDEP-2 cells with biallelic, in-frame excision of ZnF0 lacked steady-state protein level of BCL11A, as detected by Western blotting. BCL11A knockout (KO) clone was included as a control. GAPDH, glyceraldehyde-3-phosphate dehydrogenase. (**E**) Percentage of γ-globin mRNA to total non–α-globin mRNAs was determined by reverse transcription quantitative polymerase chain reaction (RT-qPCR) analysis in WT, KO, and two independent ΔZnF0 clones on day 7 of differentiation. Error bars represent SD. *n* = 2 biological replicates and each with 3 technical replicates.

erythroid cells, the protein appears stable with a half-life of ~20 hours (*22*).

To characterize full-length (FL) BCL11A (also termed BCL11A-XL), we generated recombinant protein in the baculovirus expression system. Under denaturing conditions, BCL11A migrated just above the 100-kDa marker (fig. S1C). By native gel electrophoresis and size-exclusion chromatography (SEC), FL protein behaved as a much larger species, consistent with a multimer state (fig. S1, D and E). Study of patients with pathogenic missense mutations previously suggested that BCL11A self-interacts and possibly physically associates with BCL11B when they are coexpressed (*35*, *36*). To map self-interaction domains in a systematic fashion, we coexpressed domain-deleted Myc- and green fluorescent protein (GFP)–tagged BCL11A cDNA constructs in human embryonic kidney (HEK) 293T cells and performed reciprocal immunoprecipitation (Fig. 1, A and B). These experiments indicated that ZnF0 serves as the principal domain mediating interactions (Fig. 1B). Moreover, coexpression of tagged ZnF0 constructs revealed its self-association (Fig. 1C). ZnF23 and ZnF456 failed to self-associate (fig. S2A). Additional experiments showed that FL BCL11A physically associated with a shorter isoform (BCL11A-L), and BCL11B, which has one amino acid difference in ZnF0 from that of BCL11A (fig. S2, B to D).

To study hemoglobin switching in a relevant cellular context, we used HUDEP-2 cells, an immortalized $CD34^+$-derived progenitor cell line that undergoes erythroid differentiation characterized by an adult-stage phenotype (high β-globin and low γ-globin) (*37*). As these cells can be genetically manipulated and cloned, they provide a tractable system in which to test functional requirements of specific domains in a rigorous and reproducible manner (*10*, *19*, *38*). Our experiments leverage an efficient CRISPR-Cas9 editing protocol that yields biallelically edited cells for analysis (*39*). Accordingly, transcription of the endogenous *BCL11A* loci is unperturbed upon deletion of discrete coding sequences. Independent HUDEP-2 clones lacking ZnF0 (ΔZnF0 cells) phenocopied knockout cells with respect to deficiency of steady-state protein and marked HbF reactivation (Fig. 1, D and E, and fig. S3A). *BCL11A* RNA transcripts appeared modestly increased, consistent with a degree of negative feedback repression at the *BCL11A* gene (fig. S3B) (*22*). We conclude that ZnF0 is required to maintain the steady-state level of BCL11A protein in erythroid cells.

Tetramerization is required to maintain steady-state BCL11A protein level

Upon preparation of recombinant protein, we were surprised to observe that, even at low concentrations, ZnF0 formed a stable tetramer, as assessed by velocity sedimentation centrifugation (Fig. 2A), native gel electrophoresis, and dynamic light scattering (fig. S4, A and B). The structure of crystallized ZnF0, as determined by x-ray diffraction at 1.8-Å resolution, revealed a symmetric tetramer with a hydrophobic core (Fig. 2B). At the interface where diagonal monomers meet, Leu^{57}, Ile^{60}, and Leu^{61} engage in hydrophobic interactions (Fig. 2B). Gly^{58} forms a hydrogen bond with a water molecule, which serves effectively as a bridge to stabilize the β sheets (Fig. 2B). In addition to these hydrophobic interactions, the formation of intermolecular antiparallel β sheets is facilitated by a network of hydrogen bonds between pairs of residue backbones across strands, including Leu^{45}, Leu^{46}, and Thr^{47} (Fig. 2C). Within a ZnF0 monomer, the hydrophobic residues Leu^{57}, Ile^{60}, Leu^{61}, Phe^{63}, and Ile^{64} constitute a core crucial for tetramer assembly (Fig. 2D). Structures predicted by AlphaFold 3 were similar with minor differences (fig. S4, D and E).

Downloaded from https://www.science.org at University Van Amsterdam on April 13, 2025

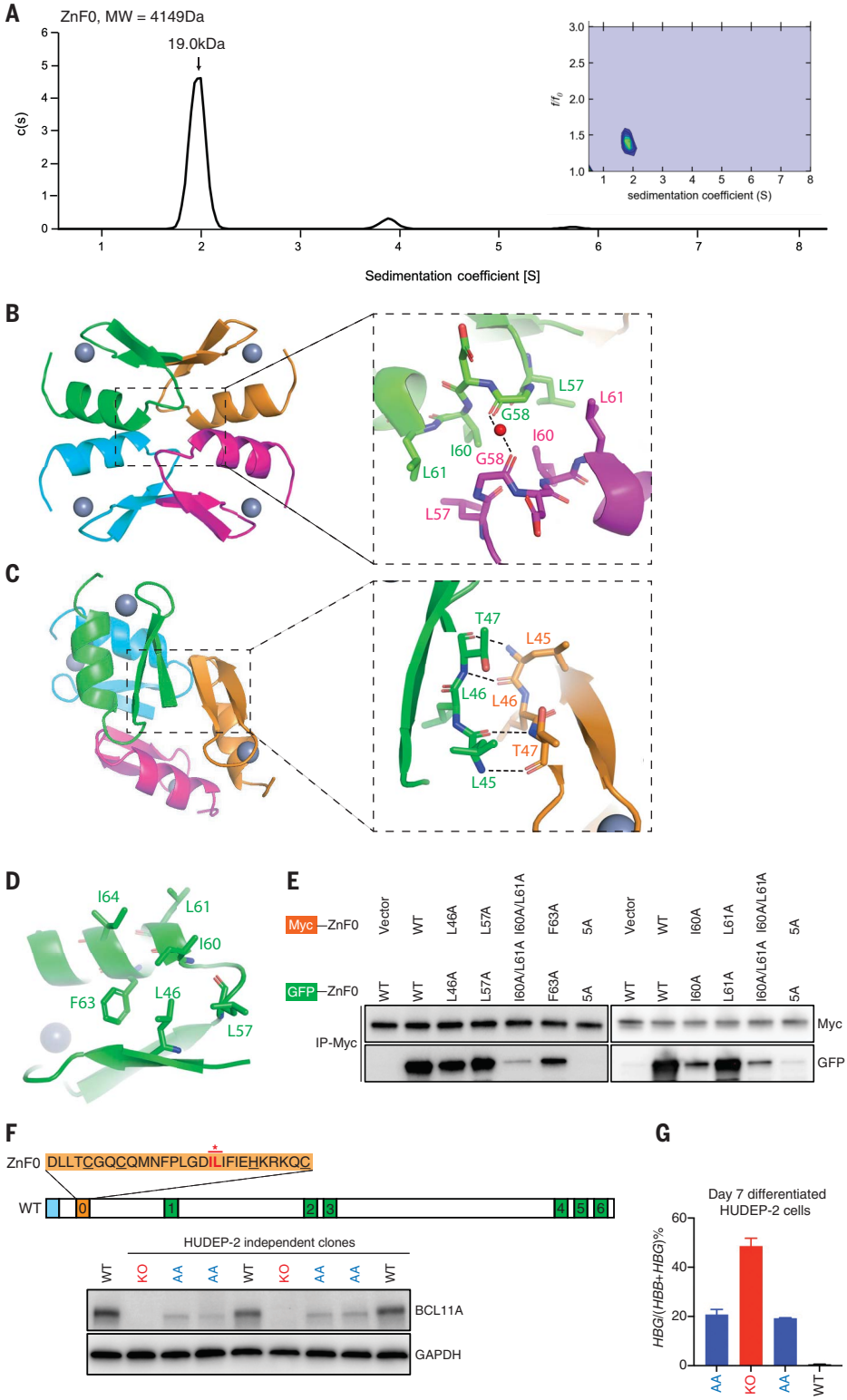

Fig. 2. Tetramerization of BCL11A is required for steady-state protein level. (**A**) c(s) distribution and two-dimensional (2D) shape and size distribution plot of ZnF0 protein by analytical ultracentrifugation (AUC) analysis. The major peak at an S value of 2S corresponds to ~19 kDa, the molecular weight of a tetramer of ZnF0 protein. MW, molecular weight. (**B**) Crystal structure of the ZnF0 tetramer. Each subunit in the tetramer is shown with a different color. Interactions between diagonally positioned monomers are labeled. The gray balls represent zinc ions (Zn^{2+}). (**C**) Interacting residues on intermolecular β sheets are shown. The gray balls represent zinc ions (Zn^{2+}). (**D**) Hydrophobic core residues within a monomer are highlighted. The gray ball represents zinc ion (Zn^{2+}). (**E**) Anti-Myc IPs were blotted with the indicated antibodies in HEK293T cells cotransfected with the indicated plasmids. 5A, five sites mutated to alanines (L46A/L57A/I60A/L61A/F63A). (**F**) I60 and L61 in ZnF0 of BCL11A were replaced with alanines (indicated by *) by CRISPR-Cas9 editing in HUDEP-2 cells. BCL11A levels in independent WT, KO, or I60A/L61A clones were analyzed by Western blotting. After CRISPR-Cas9 editing, two clones with BCL11A unmodified (WT) and two clones with BCL11A premature termination (KO) were included as controls. I60A/L61A mutations led to loss of steady-state BCL11A protein. (**G**) Percentage of γ-globin mRNA to total non–α-globin mRNAs was determined by RT-qPCR analysis on day 7 of differentiation. AA, I60A/L61A. Error bars represent SD. n = 1 with 3 technical replicates. Single-letter abbreviations for the amino acid residues are as follows: A, Ala; C, Cys; D, Asp; E, Glu; F, Phe; G, Gly; H, His; I, Ile; K, Lys; L, Leu; M, Met; N, Asn; P, Pro; Q, Gln; R, Arg; S, Ser; T, Thr; V, Val; W, Trp; and Y, Tyr.

Guided by the structure, we mapped residues critical for ZnF0 assembly by transfection of cDNA constructs in HEK293T cells (Fig. 2E). Alanine replacement of five hydrophobic residues at the tetramer interface abolished self-interaction (Fig. 2E). The alanine mutants disrupt the ZnF0 tetrameric structure, a finding consistent with the AlphaFold 3 prediction. Replacement of different combinations of residues identified isoleucine 60 (I60), a contact residue in the structure, as critical for tetramer assembly (Fig. 2E). To ascertain its role in stabilization of BCL11A in an erythroid cell context, we engineered HUDEP-2 cells with alanine replacements at

Downloaded from https://www.science.org at University Van Amsterdam on April 13, 2025

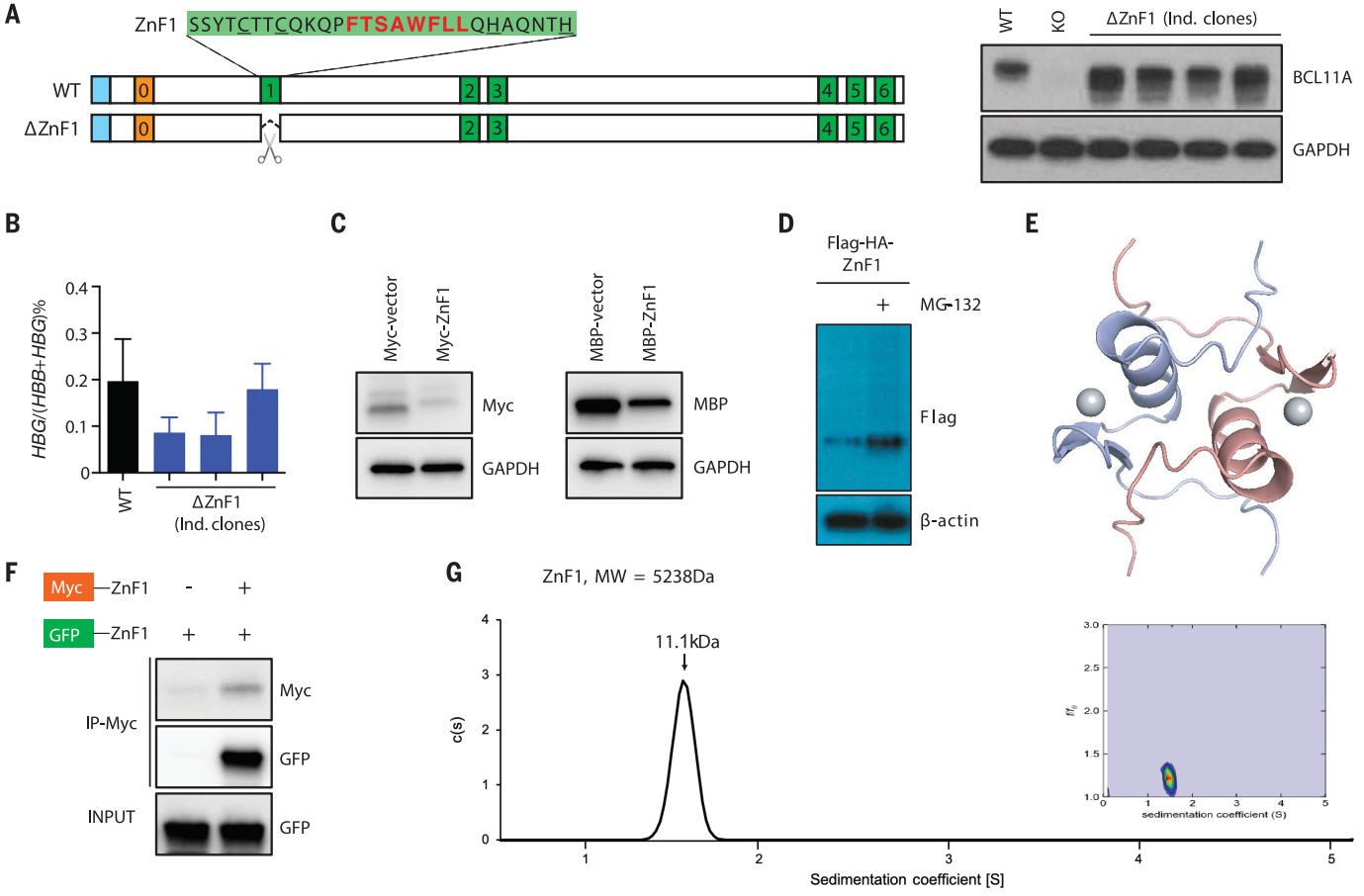

Fig. 3. Tetramerization of BCL11A facilitates dimerization of ZnF1 and shields a degron. (**A**) BCL11A ZnF1 domain contains a putative degron sequence highlighted in red. (Right) HUDEP-2 cells with biallelic excision of ZnF1 showed an elevated BCL11A level, as detected by Western blotting. BCL11A KO clone was included as a control. (**B**) RT-qPCR analysis revealed the percentage of γ-globin mRNA to total non–α-globin mRNAs in the indicated HUDEP-2 cells on day 7 of differentiation. The ΔZnF1 cells displayed a lower percentage of γ-globin in comparison with the WT cells. Error bars represent SD. *n* = 3 biological replicates. (**C**) HEK293T cells were transfected with the indicated plasmids, and cell lysates were blotted with the indicated antibodies. ZnF1 conferred instability on heterologous proteins, Myc and MBP. (**D**) Lysates of HEK293T transfected with ZnF1 in fusion with Flag-hemagglutinin (HA) tag were blotted with anti-Flag antibody. Ectopic expressed Flag-HA-ZnF1 was stabilized by the addition of the proteasome inhibitor MG-132. (**E**) Predicted dimer structure of extZnF1 by AlphaFold 3. (**F**) Anti-Myc IPs were blotted with the indicated antibodies in HEK293T cells cotransfected with the indicated plasmids. (**G**) c(s) distribution and 2D shape and size distribution plot of extZnF1 protein by AUC analysis. The major peak at an S value of 1.50S corresponds to ~11 kDa, the molecular weight of a dimer of extZnF1 protein.

I60 and the neighboring residue L61 (Fig. 2F). Independent I60A/L61A clones exhibited markedly reduced steady-state BCL11A protein (Fig. 2F) accompanied by derepression of the γ-globin gene (Fig. 2G and fig. S4F). BCL11A RNA transcript levels in the I60A/L61A clones were modestly increased (fig. S4G). The level of BCL11A I60A/L61A protein was deficient throughout the course of erythroid differentiation (fig. S4H). Taken together, these findings strongly suggest that the tetramer state of ZnF0 per se, rather than the mere presence of ZnF0, is required for production of steady-state BCL11A protein. By contrast, reported pathogenic missense mutations in ZnF0 (*35*, *36*) involve residues that directly coordinate zinc ions or neighboring residues. These pathogenic mutations also fail to form a stable tetramer, as assessed by immunoprecipitation or native gel electrophoresis (fig. S4, I and J).

Tetramerization shields BCL11A from degradation

If the native state of BCL11A is a tetramer, what is the fate of BCL11A protein expressed by ΔZnF0? Treatment of ΔZnF0 cells with the proteasome inhibitor MG-132 was accompanied by partial restoration of steady-state protein levels with time (fig. S5A), suggesting that ΔZnF0 protein was actively degraded by the ubiquitin-proteasome system. We hypothesized that a degron sequence elsewhere in ΔZnF0 protein was exposed in monomeric BCL11A and obscured in the tetramer. In contrast to findings in ΔZnF0 cells, biallelic excision of ZnF1 led to a marked increase in steady-state protein (Fig. 3A), providing evidence that ZnF1 serves a destabilizing role. BCL11A RNA transcripts in ΔZnF1 cells were not significantly changed (fig. S5B). In ΔZnF1 cells, γ-globin expression was similar to, or perhaps somewhat hyperrepressed, as compared to wild-type (WT) cells (Fig. 3B and fig. S5C). Thus, protein lacking ZnF1 retained strong repressor activity. We noted that ZnF1 contains a central stretch of hydrophobic residues (FTSAWFLL) reminiscent of known degrons (Fig. 3A) (*40*, *41*). We, therefore, tested whether degron activity was transferable to a heterologous protein. Fusion of ZnF1 with well-folded proteins, such as Myc or maltose-binding protein (MBP), reduced protein levels in transfected HEK293T cells (Fig. 3C). The level of ZnF1 expression was restored by addition of the proteasome inhibitor MG-132 (Fig. 3D). Structure prediction of ZnF1 with N- and C-terminal

Downloaded from https://www.science.org at University Van Amsterdam on April 13, 2025

extensions (extZnF1) by AlphaFold 3 suggested that extZnF1 forms a dimer with the hydrophobic stretch buried at the interface (Fig. 3E). Consistent with dimer formation, coexpression of Myc- and GFP-tagged extZnF1 constructs and immunoprecipitation in HEK293T revealed self-association (Fig. 3F). To examine its properties directly, we expressed recombinant extZnF1. We observed that, unlike ZnF23 or ZnF456, extZnF1 formed a stable dimer at low concentration, as assessed by velocity sedimentation centrifugation (Fig. 3G) and SEC–multiangle light scattering (MALS) (fig. S5D).

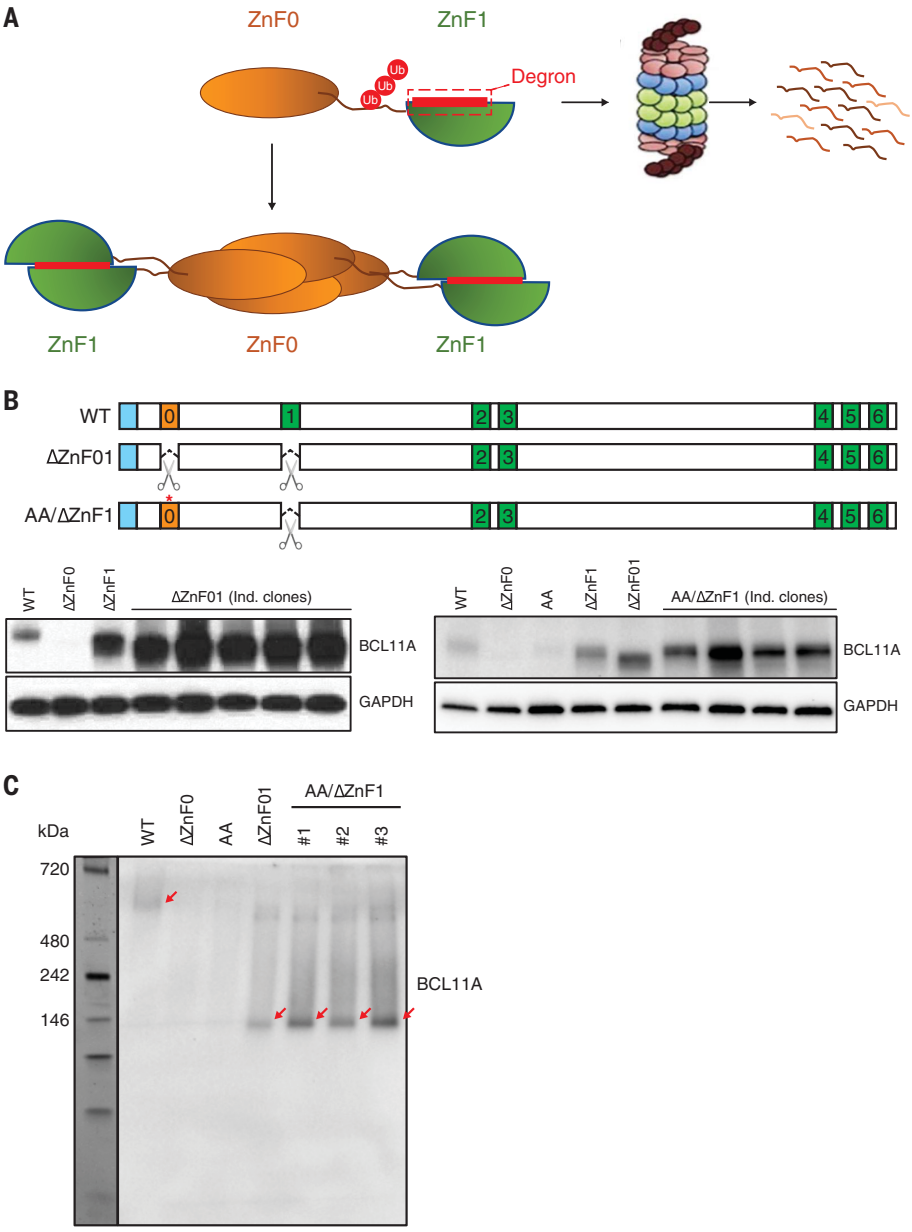

Fig. 4. BCL11A lacking ZnF0 and ZnF1 is a stable monomer. (**A**) Model depicts ZnF0-mediated BCL11A self-tetramerization as essential for production of steady-state protein. BCL11A monomer is unstable as the putative degron in ZnF1 is exposed, thereby rendering protein susceptible to proteasomal degradation. Tetramerization of ZnF0 facilitates dimerization of ZnF1, which masks the ZnF1 degron. The model posits that assembly of the ZnF0 tetramer protects BCL11A from proteasomal degradation. (**B**) HUDEP-2 cells were engineered with discrete, in-frame deletion of both ZnF0 and ZnF1 (ΔZnF01) or engineered with replacement of I60 and L61 to alanines together with deletion of ZnF1 (AA/ΔZnF1) within FL BCL11A. The steady-state protein levels of BCL11A ΔZnF01 and AA/ΔZnF1 were assessed by Western blotting. ΔZnF0, ΔZnF1, and I60A/L61A clones were included as controls. (**C**) Nuclear extractions from the indicated HUDEP-2 cells were incubated with 2.5% Triton X-100 and 5% 1,6-hexanediol for 30 min to disrupt interactions mediated by regions other than ZnF0 and ZnF1 in BCL11A and then were subjected to native polyacrylamide gel electrophoresis (PAGE) and blotted with anti-BCL11A antibody. The arrows indicate the expected positions of WT and mutant BCL11A proteins. BCL11A ΔZnF0 and I60A/L61A were below detection, despite MG-132 treatment of cells.

Combined deletion of ZnF0 and ZnF1 creates a monomeric BCL11A protein

To account for the contrasting findings upon deletion of ZnF0 or ZnF1, we propose a model for steady-state BCL11A protein production (Fig. 4A). As first translated, BCL11A is susceptible to proteasomal degradation owing to the presence of an exposed degron in ZnF1. Tetramerization of BCL11A driven by ZnF0 facilitates dimerization of ZnF1, thereby shielding its internal degron (*41*–*43*). Multimeric BCL11A is thereby rendered resistant to proteasomal degradation, consistent with its long half-life in cells (*22*).

If ZnF1 harbors the sole strong degron in BCL11A, expression of protein discretely lacking both ZnF0 and ZnF1 should be stable, despite an inability to assume a tetramer state. We confirmed that removal of both ZnF0 and ZnF1 abolished multimer assembly in HEK293T cells cotransfected with Myc- and GFP-tagged versions of BCL11A (fig. S6A). Native BCL11A protein lacking ZnF0 and ZnF1 migrated at the size of a monomer by native gel electrophoresis (fig. S6B). A similar result was observed with a combination of tetrameric-deficient mutation(s) and removal of ZnF1 (fig. S6, A and B). We next engineered HUDEP-2 cells with biallelic deletions of both ZnF0 and ZnF1 (ΔZnF01), as well as cells with I60A/L61A in the context of ZnF1 deletion (AA/ΔZnF1) (Fig. 4B). Independent ΔZnF01 and AA/ΔZnF1 clones exhibited elevated levels of steady-state protein (Fig. 4B). Notably, the elevated protein level in the tetramerization-deficient mutant AA/ΔZnF1 further supports the conclusion that the lack of stable BCL11A protein reflects the failure of tetramer assembly rather than a consequence of an unfolded protein response elicited by I60A/L61A mutations in ZnF0. Compared with WT BCL11A, both ΔZnF01 and AA/ΔZnF1 proteins behave as a monomer in native gels (Fig. 4C). As with other domain-deletion mutants, *BCL11A* RNA transcript levels were unaffected (fig. S6C). The half-life of ΔZnF01 BCL11A was somewhat reduced as compared with WT BCL11A (fig. S6, D and E). Production of monomeric forms of stable BCL11A in cells harboring ΔZnF01 or AA/ΔZnF1 alleles is consistent with, and supports, the proposed model (Fig. 4A). These "engineered monomers," which lack a stable tetramer structure, may be available to undergo weak interactions with other nuclear proteins, as suggested by their appearance in native gel electrophoresis (Fig. 4C and fig. S6B).

Precise genetic modification of HUDEP2 cells has been critical in dissecting the structure-function relationships of BCL11A described

Downloaded from https://www.science.org at University Van Amsterdam on April 13, 2025

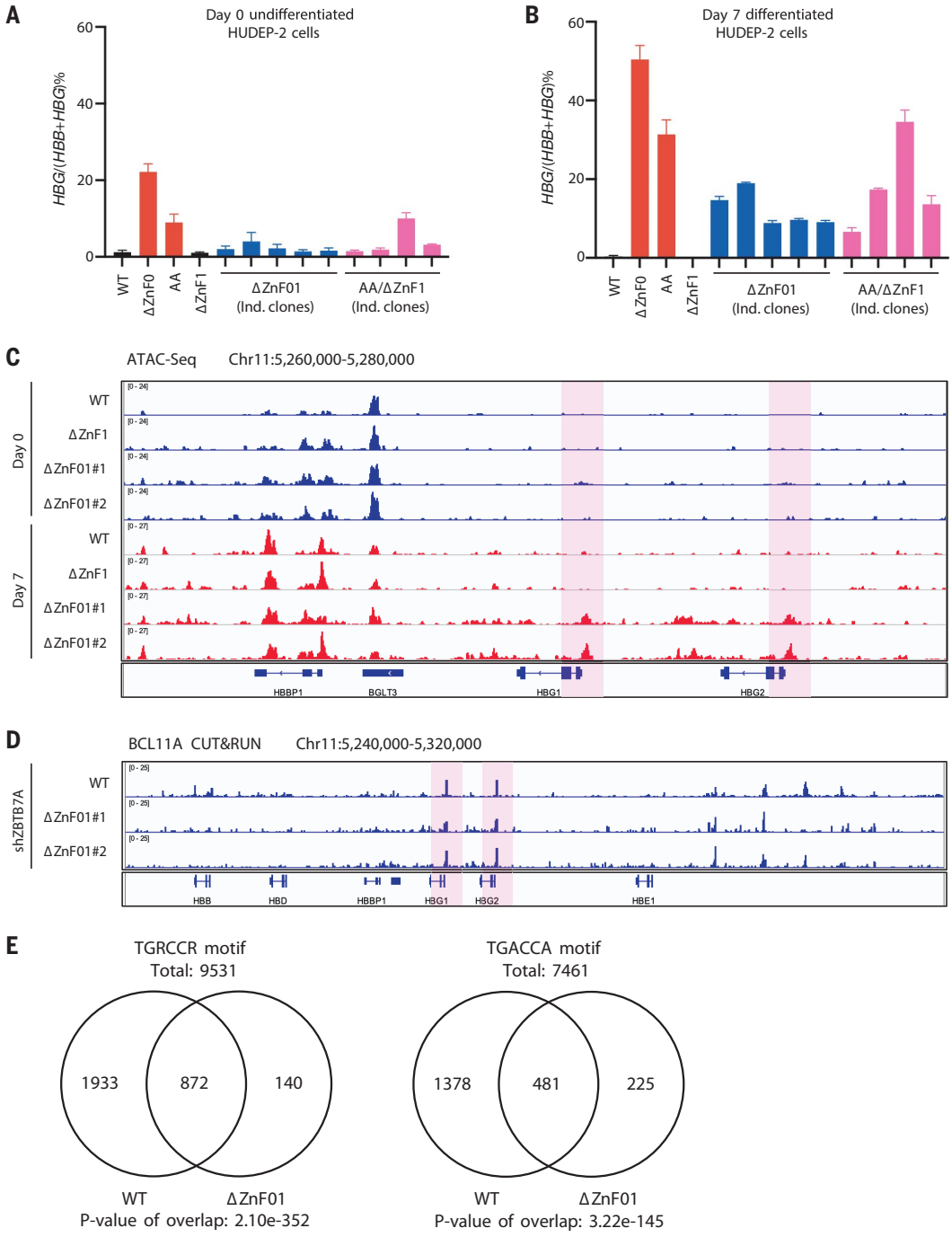

Fig. 5. Engineered monomeric BCL11A is defective in γ-globin repression. (**A**) RT-qPCR analysis showed the percentage of γ-globin mRNA to total non–α-globin mRNAs in undifferentiated HUDEP-2 cells. Error bars represent SD. *n* = 4 biological replicates for WT and ΔZnF01#3; *n* = 3 biological replicates for ΔZnF1; *n* = 2 biological replicates for ΔZnF0 and the rest of the ZnF01 clones; and *n* = 1 with 3 technical replicates for AA and AA/ΔZnF1 clones. (**B**) Similar analysis on day 7 of differentiation. Error bars represent SD. *n* = 3 biological replicates for WT; *n* = 2 biological replicates for ΔZnF0, ΔZnF1, and ΔZnF01#3; and *n* = 1 with 3 technical replicates for the rest of ΔZnF01 clones, AA and AA/ΔZnF1 clones. (**C**) Chromosome accessibility at the β-globin locus in the indicated HUDEP-2 cells was assessed by ATAC-Seq, on days 0 and 7 of differentiation. For each sample, three biological replicates were performed, and the signals were combined to generate tracks. The γ-globin promoter regions are highlighted in pink. (**D**) WT and ΔZnF01 HUDEP-2 cells transduced with lentivirus carrying ZBTB7A shRNA were subjected to BCL11A CUT&RUN analysis on day 7 of differentiation. BCL11A occupancy at the γ-globin promoters is highlighted in pink. (**E**) Venn diagrams of genome-wide colocalization of BCL11A peaks that contain TGRCCR or TGACCA motif in WT and ΔZnF01 HUDEP-2 cells. The total numbers of each motif in the genome are shown.

here. Given the intrinsic property of ZnF0 to self-assembly as a tetramer, it seemed likely that BCL11A protein behaves similarly in all cells in which BCL11A is expressed. To assess the state of endogenous BCL11A in short-lived, primary CD34$^+$ HSPCs, we expressed constructs containing ZnF0+ZnF1 (cDNA spanning both ZnFs, ZnF01) and observed that ZnF01 increased the level of steady-state protein, consistent with assembly into newly synthesized multimeric protein (fig. S7A). Furthermore, expression of ZnF01 linked to an Fc domain attenuated this increase owing to degradation of ZnF01 or the assembled complex by TRIM-away (fig. S7A) (*44*). By native gel electrophoresis, endogenous BCL11A in primary CD34$^+$ HSPCs and immortal B-lymphoid cells of the JeKo-1 line (*45*) behaved as a high molecular weight species similar to that in HUDEP-2 cells (fig. S7, B and C). These findings strongly suggest that the multimeric state of BCL11A is similar in all cells, because it is driven by the intrinsic property of ZnF0 to form a tetramer.

Tetramerization of BCL11A is critical for γ-globin repression

ΔZnF01 and AA/ΔZnF1 cells afford the opportunity to assess the contribution of tetramer formation and multivalency to γ-globin repression, independent of the role of ZnF0 in production of steady-state protein. To test the function of engineered monomeric BCL11A,

Downloaded from https://www.science.org at University Van Amsterdam on April 13, 2025

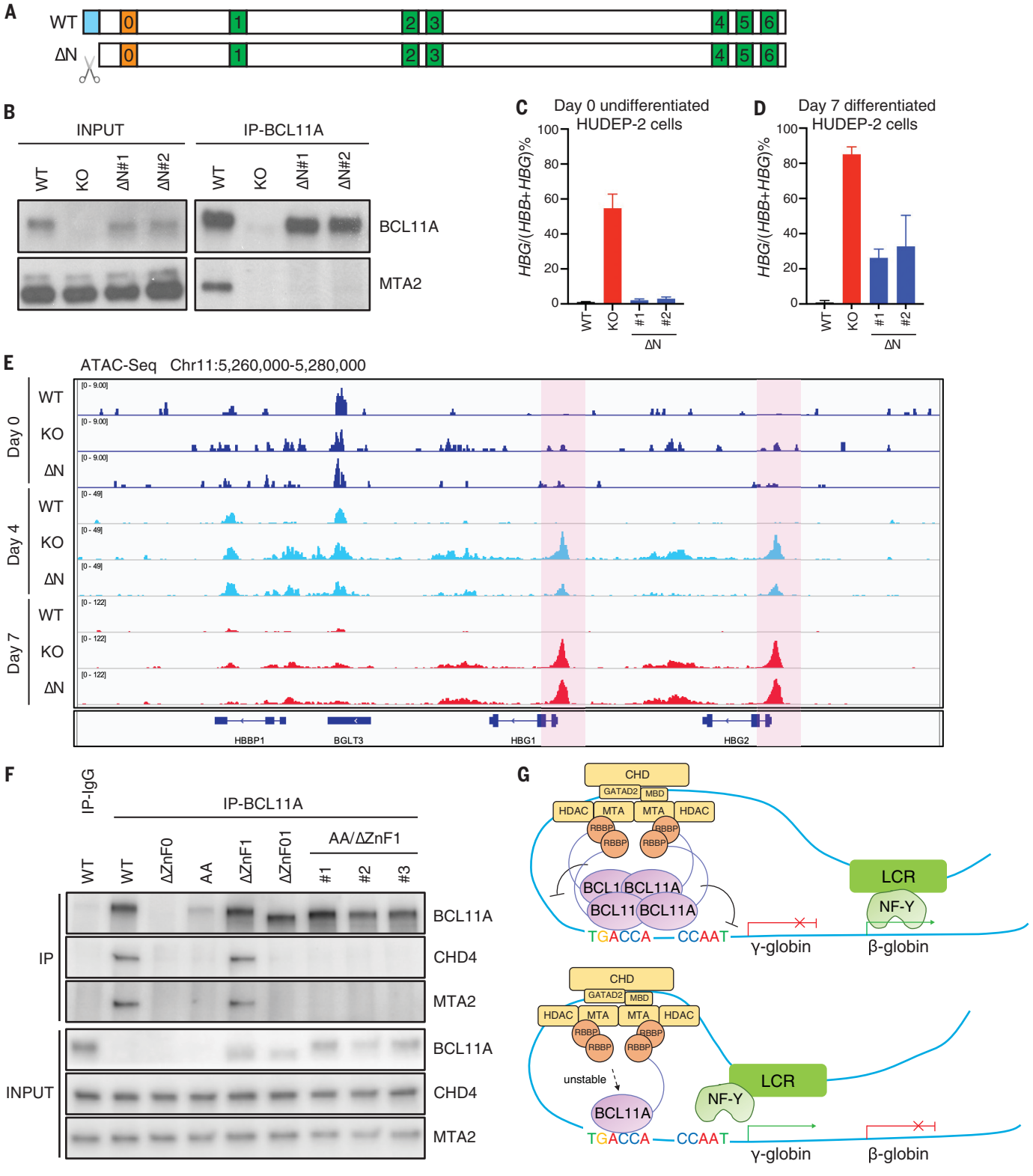

Fig. 6. Monomeric BCL11A is defective for stable NuRD engagement. (**A**) Schematic of biallelic excision of the N-terminal NuRD-binding domain in BCL11A in HUDEP-2 cells by CRISPR-Cas9 editing. (**B**) Total cell lysates (INPUT) and anti-BCL11A IPs were blotted with the indicated antibodies in WT, KO, and ΔN HUDEP-2 cells. (**C**) RT-qPCR analysis showed the percentage of γ-globin mRNA to total non–α-globin mRNAs in the indicated undifferentiated HUDEP-2 cells. Error bars represent SD. *n* = 2 biological replicates and each with 3 technical replicates. (**D**) Similar analysis on day 7 of differentiation. Error bars represent SD. *n* = 2 biological replicates and each with 3 technical replicates. (**E**) Chromosome accessibility at the β-globin locus in the indicated HUDEP-2

Downloaded from https://www.science.org at University Van Amsterdam on April 13, 2025

cells was assessed by ATAC-Seq on days 0, 4, and 7 of differentiation. Two replicates of day 0 and 4 samples and three replicates of day 7 samples were performed, and the signals were combined to generate tracks. The γ-globin promoter regions are highlighted in pink. (**F**) Total cell lysates (INPUT) and anti–immunoglobulin G (IgG) and anti-BCL11A IPs were blotted with the indicated antibodies in WT and engineered ΔZnF0, I60A/L61A, ΔZnF1, ΔZnF01, and AA/ΔZnF1 HUDEP-2 cells. (**G**) Model depicting the role of the BCL11A tetramer in repression. In WT adult-stage erythroid cells, the BCL11A tetramer stably engages the NuRD complex in a concerted fashion and prevents NF-Y binding by steric hindrance to repress γ-globin expression. However, although capable of binding the TGACCA motif at the γ-globin promoters, BCL11A monomer fails to stably engage NuRD and, because of its overall smaller size, is unable to displace NF-Y. Both features may contribute to a defect in repression. HDAC, histone deacetylase.

we examined globin levels on days 0 and 7 of differentiation (Fig. 5, A and B). Despite elevated steady-state protein, cells expressing ΔZnF01 or AA/ΔZnF1 BCL11A exhibited a defect in HbF silencing, principally upon differentiation at which time globin expression is robust. The levels of both γ-globin RNA and HbF protein were substantially elevated as compared with WT and ΔZnF1 cells (Fig. 5B and fig. S8, A and B). Consistent with these findings, chromosome accessibility at the γ-globin promoters was increased in differentiated ΔZnF01 cells, as assessed by ATAC-Seq analysis (Fig. 5C) (*46*). These results demonstrate that monomeric ΔZnF01 BCL11A is defective for HbF silencing. Thus, tetramerization of BCL11A is critical for proper γ-globin repression.

Monomeric BCL11A exhibits defects in chromatin occupancy and NuRD complex engagement

In seeking to uncover how monomeric ΔZnF01 BCL11A differs from tetramer BCL11A in repression, we first assessed occupancy at the γ-globin promoter. Despite its location at the C terminus of BCL11A, we sought to exclude the possibility that the ZnF456 DNA binding domain might be occluded. We performed BCL11A CUT&RUN (*47*) in WT and ΔZnF01 HUDEP-2 cells. In WT cells, the γ-globin locus is highly repressed, and virtually inaccessible, as assessed by ATAC (Fig. 5C) (*46*). To render the locus more accessible and permit BCL11A antibody penetration, we performed CUT&RUN in cells depleted of ZBTB7A/LRF. As shown in Fig. 5D, occupancy at the γ-globin promoters appeared similar between ΔZnF01 and WT cells. Hence, we infer that monomeric ΔZnF01 BCL11A is competent to bind to its target site in the γ-globin promoters. Consistent with a defect in repression, however, ΔZnF01 protein failed to fully evict NF-Y at the locus (fig. S8C). To assess chromatin occupancy more broadly, we enumerated CUT&RUN peaks genome-wide at both consensus (TGRCCR) and cognate (TGACCA) BCL11A binding motifs. We observed extensive and highly significant overlap of peaks between WT and ΔZnF01 (Fig. 5E). Despite the increased level of ΔZnF01 protein, however, the number of peaks was modestly reduced, suggesting that the monomer may be less able to occupy, or be retained, at target sites. Genome-wide analysis also showed that ΔZnF01 exhibited a weakened motif footprint compared to WT (fig. S8D). Taken together, these findings indicate that engineered monomeric BCL11A occupies chromatin at its target sites and therefore retains DNA binding capacity, but aspects of its function may be attenuated relative to normal BCL11A protein in chromatin.

A canonical N-terminal peptide sequence of BCL11A engages the NuRD complex through interaction with RBBP4 (*30*, *32*). Prior genetic analysis established a functional role for specific NuRD subunits in HbF silencing (*31*). To assess BCL11A-dependent NuRD engagement, we removed the NuRD-binding sequence in HUDEP-2 cells by biallelic gene editing (Fig. 6A). As anticipated, ΔN BCL11A-expressing cells failed to interact with the NuRD complex, as assessed by immunoprecipitation for the MTA2 subunit (Fig. 6B). Despite expression of BCL11A protein (fig. S8A), HbF repression was impaired in differentiated cells (Fig. 6, C and D, and fig. S9, B to D). In undifferentiated cells, which express globin transcripts at a low level, the fraction of γ-globin transcripts was not significantly increased compared with WT cells. In agreement with these observations, accessibility at the γ-globin promoters was increased only upon differentiation (Fig. 6E). Thus, consistent with prior inferences, we validated that BCL11A-dependent NuRD engagement is required for proper HbF silencing.

The similar phenotypes of ΔZnF01 and AA/ΔZnF1 with ΔN BCL11A-expressing cells led us to examine engagement of the NuRD complex in cells expressing monomeric BCL11A. As shown in Fig. 6F, interaction of ΔZnF01 or AA/ΔZnF1 with NuRD was markedly impaired, as revealed by coimmunoprecipitation for CHD4 and MTA2. In chromatin analyses, we observed occupancy of MTA2 at the HBB and HBD loci, which was attenuated, as expected, in ΔN cells (fig. S9E). Occupancy of MTA2 appeared similarly reduced in ΔZnF01 cells (fig. S9F). The severe deficit in NuRD complex engagement of monomeric protein in cells, despite the presence of a single NuRD-binding motif, further underscores the critical role of the tetramer in BCL11A function. We infer that monomeric BCL11A is defective in repression at the γ-globin locus, in part due to a deficit in NuRD complex engagement.

Discussion

Our principal finding that ZnF0-mediated tetramerization of BCL11A is necessary for both production of steady-state protein and proper silencing of HbF provides new perspectives on the native state of BCL11A and its function, as well as on opportunities for possible therapeutic intervention.

Transcription factors are often found in dimers or higher-order complexes (*48*). Most commonly, such multimers establish a high-affinity binding domain, as illustrated by dimeric basic helix-loop-helix (bHLH) factors (*49*) or tetrameric p53 protein (*50*). Although ZnFs are typically viewed as DNA binding domains, they also participate in protein-protein interactions, such as in GATA (*51*) and Ikaros factors (*52*). To our knowledge, however, BCL11A protein presents a distinct example in which multivalency is established by a ZnF that forms a stable tetramer within an otherwise largely unstructured protein. In effect, tetramerization is "hardwired" in BCL11A, as well as its close paralog BCL11B, and therefore likely characterizes the protein in all cells in which it is expressed. Our findings in primary CD34+ HPSCs and a B cell line support this inference (fig. S7C). Although we have found that tetramer formation is critical, the nature of protein complexes of BCL11A is likely more complex, as suggested by its behavior in native gels (see Fig. 4C and figs. S4J, S6B, and S7, B and C). For example, dimer formation driven by ZnF1 may bring together BCL11A polypeptides of different tetramers, thereby generating a lattice of protein. Other studies will be required to address these possibilities.

Tetramerization via ZnF0 serves a critical function in stabilization of BCL11A protein by preventing proteasomal degradation of monomers through shielding a degron located in ZnF1 (*41*). The intrinsic property of recombinant ZnF1 to form dimers suggests that ZnF0 tetramerization promotes ZnF1 dimerization, perhaps during protein translation. Further studies are needed to define the structure of ZnF1 dimers, identify the E3 ubiquitin ligase (s) that act on the degron, and establish how events are coordinated as nascent peptides are synthesized. Expression of stable monomeric ΔZnF01 indicates that no other strong degrons reside elsewhere in BCL11A. Taken together, the pathway of stabilization we describe for BCL11A protein likely accounts for its long half-life in cells.

Besides its role in controlling protein stability, tetramerization confers additional properties

Downloaded from https://www.science.org at University Van Amsterdam on April 13, 2025

to BCL11A that affect chromatin occupancy and co-repressor engagement. Engineered monomeric BCL11A occupies chromatin at target sites but seems to do so less well than WT protein (Fig. 5E). The precise basis for this apparent deficit is unclear. Current methods do not allow for quantitative assessment of relative affinities of multimeric protein complexes for DNA. The observed differences in genome-wide chromatin occupancy may reflect the deficit in engagement of the NuRD complex by monomeric ΔZnF01. Taken together, our findings indicate that the tetramer state is required to ensure assembly of a repressive environment at the promoter. Cryo–electron microscopy studies and stoichiometry experiments indicate that each NuRD complex bears four RBBP4 subunits (*32*), which corresponds, either by chance or evolutionary design, to the four NuRD-binding sequences on a BCL11A tetramer. Concerted engagement of NuRD by the tetramer may anchor NuRD complexes more stably than a monomer within large protein complexes at the γ-globin promoters. Previously, we presented evidence that BCL11A or unrelated proteins (such as dCas9) act as a steric barrier to NF-Y binding at the proximal CCAAT motif in the γ-globin promoters (*10*). Weaker eviction of NF-Y by ΔZnF01 because of its overall smaller size may also contribute to impaired repression. We propose an updated model for repression at the γ-globin promoter in which tetrameric BCL11A cooperatively engages the NuRD complex in a stable fashion (Fig. 6G). The extent to which transcription factor multivalency, as described here, is a special feature evolved for repression is unknown. Although γ-globin repression is reversed by removal of BCL11A (or ZBTB7A), the γ-globin loci are inaccessible (as assessed by ATAC) in adult-type erythroid precursors. We speculate that the multivalent state of BCL11A contributes to occlusion of the locus.

BCL11A is a modular protein composed of seven ZnFs, a NuRD-binding sequence, and large disordered regions. As such, the protein lacks structured domains for identification of small-molecule ligands that serve as starting points for therapeutic development of inhibitors or protein degraders. Whether more tractable protein targets for HbF reactivation remain to be identified is uncertain. Given that BCL11A acts proximally in γ-globin repression (*9*, *10*) and has been validated clinically as a target (*21*, *23*), efforts targeted to the protein offer the best prospect for mechanism-based therapy. Our findings regarding the expression and assembly of BCL11A protein identify vulnerabilities that present unforeseen opportunities for therapeutic intervention. Tetramer formation mediated by ZnF0 constitutes a vulnerability for HbF repression. Agents that prevent or disrupt tetramerization would lead to down-regulation of BCL11A protein and relieve HbF silencing. Similarly, agents that perturb dimerization of ZnF1 would also promote proteasomal degradation of BCL11A. However, the tetramer structure of ZnF0 provides a stable domain in an otherwise largely disordered protein. Although assembled from a ZnF, the overall structure of the tetramer is distinct from that of ZnF domains. Discovery of ligands that bind the tetramer surface may represent a starting point for small molecules to down-modulate BCL11A protein in a therapeutic context.

REFERENCES AND NOTES

1. S. H. Orkin, *Med* **2**, 122–136 (2021).
2. J. Watson, *Am. J. Med. Sci.* **215**, 419–423 (1948).
3. S. Menzel *et al*., *Nat. Genet.* **39**, 1197–1199 (2007).
4. M. Uda *et al*., *Proc. Natl. Acad. Sci. U.S.A.* **105**, 1620–1625 (2008).
5. F. S. Collins *et al*., *Nature* **313**, 325–326 (1985).
6. R. Gelinas, B. Endlich, C. Pfeiffer, M. Yagi, G. Stamatoyannopoulos, *Nature* **313**, 323–325 (1985).
7. V. G. Sankaran *et al*., *Science* **322**, 1839–1842 (2008).
8. G. E. Martyn *et al*., *Nat. Genet.* **50**, 498–503 (2018).
9. N. Liu *et al*., *Cell* **173**, 430–442.e17 (2018).
10. N. Liu *et al*., *Nat. Genet.* **53**, 511–520 (2021).
11. X. Yu *et al*., *Haematologica* **104**, 2361–2371 (2019).
12. F. Grosveld, G. B. van Assendelft, D. R. Greaves, G. Kollias, *Cell* **51**, 975–985 (1987).
13. W. Deng *et al*., *Cell* **149**, 1233–1244 (2012).
14. T. Masuda *et al*., *Science* **351**, 285–289 (2016).
15. D. E. Bauer *et al*., *Science* **342**, 253–257 (2013).
16. A. Basak *et al*., *J. Clin. Invest.* **125**, 2363–2368 (2015).
17. C. Brendel *et al*., *J. Clin. Invest.* **126**, 3868–3878 (2016).
18. J. Xu *et al*., *Science* **334**, 993–996 (2011).
19. M. C. Canver *et al*., *Nature* **527**, 192–197 (2015).
20. J. Vierstra *et al*., *Nat. Methods* **12**, 927–930 (2015).
21. H. Frangoul *et al*., *N. Engl. J. Med.* **384**, 252–260 (2021).
22. S. Mehta *et al*., *Cell Chem. Biol.* **29**, 1273–1287.e8 (2022).
23. E. B. Esrick *et al*., *N. Engl. J. Med.* **384**, 205–215 (2021).
24. A. Rivers, R. Jagadeeswaran, D. Lavelle, *Am. J. Physiol. Regul. Integr. Comp. Physiol.* **315**, R840–R847 (2018).
25. S. Cui *et al*., *Blood* **126**, 386–396 (2015).
26. R. Molokie *et al*., *PLOS Med.* **14**, e1002382 (2017).
27. A. Renneville *et al*., *Blood* **126**, 1930–1939 (2015).
28. P. Y. Ting *et al*., *Science* **385**, 91–99 (2024).
29. J. E. Bradner *et al*., *Proc. Natl. Acad. Sci. U.S.A.* **107**, 12617–12622 (2010).
30. S. Lejon *et al*., *J. Biol. Chem.* **286**, 1196–1203 (2011).
31. F. Sher *et al*., *Nat. Genet.* **51**, 1149–1159 (2019).
32. S. Arvindekar *et al*., *Protein Sci.* **31**, e4387 (2022).
33. B. Xue, R. L. Dunbrack, R. W. Williams, A. K. Dunker, V. N. Uversky, *Biochim. Biophys. Acta* **1804**, 996–1010 (2010).
34. J. Abramson *et al*., *Nature* **630**, 493–500 (2024).
35. P. Grabarczyk *et al*., *Mol. Cell. Biol.* **38**, e00368–e00317 (2018).
36. Y. Shen *et al*., *PLOS Genet.* **17**, e1009835 (2021).
37. R. Kurita *et al*., *PLOS ONE* **8**, e59890 (2013).
38. P. Huang *et al*., *Nat. Genet.* **54**, 1417–1426 (2022).
39. S. Mehta, A. Buyanbat, S. Orkin, B. Nabet, *Methods Enzymol.* **681**, 1–22 (2023).
40. P. H. Kussie *et al*., *Science* **274**, 948–953 (1996).
41. M. Guharoy, T. Lazar, M. Macossay-Castillo, P. Tompa, *Commun. Biol.* **5**, 445 (2022).
42. P. R. Johnson, R. Swanson, L. Rakhilina, M. Hochstrasser, *Cell* **94**, 217–227 (1998).
43. T. Hattori, N. Ohoka, Y. Inoue, H. Hayashi, K. Onozaki, *Oncogene* **22**, 1273–1280 (2003).
44. D. Clift, C. So, W. A. McEwan, L. C. James, M. Schuh, *Nat. Protoc.* **13**, 2149–2175 (2018).
45. H. J. Jeon, C. W. Kim, T. Yoshino, T. Akagi, *Br. J. Haematol.* **102**, 1323–1326 (1998).
46. J. D. Buenrostro, B. Wu, H. Y. Chang, W. J. Greenleaf, *Curr. Protoc. Mol. Biol.* **109**, 29.1, 9 (2015).
47. P. J. Skene, S. Henikoff, *eLife* **6**, e21856 (2017).
48. P. M. C. Park *et al*., *Mol. Cell* **84**, 2511–2524.e8 (2024).
49. C. R. Vinson, P. B. Sigler, S. L. McKnight, *Science* **246**, 911–916 (1989).
50. J. Gencel-Augusto *et al*., *Cancer Discov.* **13**, 1230–1249 (2023).
51. E. H. Bresnick, K. R. Katsumura, H. Y. Lee, K. D. Johnson, A. S. Perkins, *Nucleic Acids Res.* **40**, 5819–5831 (2012).
52. A. Molnár, K. Georgopoulos, *Mol. Cell. Biol.* **14**, 8292–8303 (1994).

ACKNOWLEDGMENTS

We thank J. Hong (IGM Biosciences) and V. Hargreaves (Psivant Therapeutics) for contributions to initial characterization of BCL11A protein and D. Finley (Harvard Medical School) and A. Koehler (MIT) for helpful discussion. We also thank M. Rackham (Isomorphic Labs) for advice on structural predictions of the ZnF1 dimer. We thank the Molecular Biology Core Facility at Dana-Farber Cancer Institute and the Center for Macromolecular Interactions at Harvard Medical School. Computational analyses were conducted on the O2 high-performance computer cluster, supported by the Research Computing Group at Harvard Medical School. AUC analyses were performed at the Johnson Foundation Biophysics and Structural Biology Core at the Perelman School of Medicine with the support of an NIH High-End Instrumentation Grant (S10-OD018483). S.H.O. is an Investigator of the Howard Hughes Medical Institute. **Funding:** Research support was provided by the Doris Duke Charitable Foundation and the Howard Hughes Medical Institute. **Author contributions:** Conceptualization: G.Z., M.Y., S.M., and S.H.O. Methodology: G.Z., M.Y., S.M., I.C., and S.H.O. Investigation: G.Z., M.Y., S.M., and all authors. Visualization: G.Z., M.Y., S.M., I.C., S.W., Q.Z., and S.H.O. Funding acquisition: S.H.O. Project administration: S.H.O. Supervision: S.H.O. Writing – original draft: G.Z. and S.H.O. Writing – review and editing: G.Z., M.Y., S.M., and all authors. **Competing interests:** Authors declare that they have no competing interests. **Data and materials availability:** The crystallographic structure for ZnF0 (PDB ID 9B4P) has been deposited to the publicly accessible database Protein Data Bank available at https://www.rcsb.org/. Genomic sequencing data have been deposited to GSE263968. All other materials are available from the authors upon request. **License information:** Copyright © 2024 the authors, some rights reserved; exclusive licensee American Association for the Advancement of Science. No claim to original US government works. https://www.sciencemag.org/about/science-licenses-journal-article-reuse

SUPPLEMENTARY MATERIALS

science.org/doi/10.1126/science.adp3025
Materials and Methods
Figs. S1 to S9
Tables S1 to S3
References (*53*–*60*)
MDAR Reproducibility Checklist
Data S1 to S8

Submitted 22 March 2024; resubmitted 8 August 2024
Accepted 21 October 2024
10.1126/science.adp3025

Downloaded from https://www.science.org at University Van Amsterdam on April 13, 2025